ACCELERATED FLIGHT ENVELOPE EXPANSION USING NEAR REAL TIME STABILITY MARGIN ESTIMATION

Vijay V. Patel*, Girish Deodhare* and Shyam Chetty**

Abstract

A novel technique for estimating the stability margins in near real time has been developed by the authors [1]. This paper shares the invaluable flight test experience gained in using it for flight envelope expansion of India's first digital fly-by-wire Light Combat Aircraft (LCA). Use of this technique has resulted in reducing the overall flight test effort and cost without compromising safety.

Using the technique, it was possible to estimate the stability margins on a desktop computer using real time telemetry data within approximately 60 seconds of completing the test. The flight test results for 'Fixed' (restricted flight envelope) and 'Scheduled' (full flight envelope) gain control laws, for manually generated pilot 3-2-1-1 inputs and pre-programmed 3-2-1-1 inputs generated using the onboard Flight Test Panel (FTP) are presented.

During the LCA flights, the stability margins were found to be satisfactory throughout the flight envelope. In order to establish that the same technique would work equally well when the stability margins are marginal, typical results were also generated using simulation data and are included in this paper. By artificially increasing the plant gain / delay in the simulation model it is shown that even if the stability margins are low, the same technique correctly estimates the relative stability.

Introduction

The flight control system design is carried out using the aerodynamic data generated in wind tunnels. For an aircraft development programme, it is necessary to validate this aero data using flight tests before expanding to the boundaries of the flight envelope thereby not compromising safety. The safety and productivity of the initial flight test phase of a prototype vehicle can be enhanced by developing techniques that enable measurement of the stability margins in near real time. These techniques allow flight test personnel to minimize flight test effort as clearance for executing the next test point can be immediately given if the stability margins at the current test point are found to be satisfactory.

There are several methods proposed in literature [2, 3, 8, 9] based on Fast Fourier Transforms (FFT), Z-Transforms etc. for determining the stability margins in near real time. The techniques using purely FFT analysis are generally faster and work well if the excitation signals are sine sweeps which cover the gain / phase crossover frequency range of the closed loop aircraft. The main shortcoming of performing this analysis is the 'longer duration of the excitation signal' required for providing adequate coverage over a wide frequency range.

Methods using parameter estimation procedures postulating state variable models [4] work well with time domain inputs such as doublets or 3-2-1-1 signals (see Appendix A for the details of this signal) but are computationally intensive due to the iterative nature of the algorithms and analysis. Thus, they are ideally suited for 'off-line' accurate determination of stability and control derivatives.

During initial flight trials of a new aircraft, computer generated signal injection systems capable of exciting the aircraft with i) sine sweep signals or ii) high bandwidth

*IFCS, Aeronautical Development Agency, Vimanapura Post, Bangalore-560 017, India
Email : vvp2069@yahoo.com or girish@dishnetdsl.net
**Flight Mechanics and Computational Division (FMCD), National Aerospace Laboratories, Kodihalli, Bangalore-560 017, India
Email : shyam@css.nal.res.in
Manuscript received on 05 Sep 2005; Paper reviewed, revised and accepted on 12 Jul 2006

3-2-1-1 signals will generally not have been cleared for flight. Thus, flight data analysis has to be invariably done using manually generated piloted (low bandwidth) inputs such as 3-2-1-1 and doublets, even though sine sweeps are the preferred inputs for determining stability margins. Further the aircraft response signals due to manually generated doublets and 3-2-1-1 inputs have lower bandwidths compared to the gain and phase crossover frequencies of the 'aircraft + flight control system' loop transfer function. Typical fighter aircraft like LCA have gain and phase crossover frequencies around 1 Hz and 3 Hz respectively. The well-practiced piloted 3-2-1-1 inputs typically with an overall time duration of seven seconds have a signal bandwidth of around 1 to 1.5 Hz. Hence estimating the stability margins from these low bandwidth signals is a challenging problem and special analysis techniques are needed.

In [1], a new method combining 'FFT techniques' and 'parameter estimation in the frequency domain' has been developed to accurately determine the stability margin of the longitudinal axis of a Fly By Wire (FBW) fighter aircraft with 3-2-1-1 inputs. In fact, this technique consists of 'Three FFT Methods' with increasing order of complexity.

I. "Method I" is to find the open loop frequency response from the closed loop data. This is the most common method used in the literature. Moreover, since the energy content beyond 1Hz in the excitation signal is insufficient, the method leads to noisy frequency response estimates.

II. The controller and associated hardware transfer functions (accounting for all lags) are accurately determined experimentally in ground-based rigs. Since the controller is known a priori, it logically follows that one can estimate only the open loop plant frequency response using FFT and then concatenate it with the controller and associated hardware frequency response to obtain the loop transfer function. This technique is referred here as "Method II". The FFT is carried out based on plant input / output signals, and the signal to noise ratio deteriorates beyond 1 Hz as the energy in the excitation signal is insufficient. Consequently estimation of the phase crossover frequency and hence the gain margin tends to become inaccurate.

III. The structure of the short period aircraft transfer functions is well known [6]. The short period pitch rate (q) and normal acceleration (Nz) to elevator (δ_e) transfer functions are of second order. Thus, a parameter estimation procedure in the frequency domain based on this model structure can be used to derive a best-fit transfer function parameters from the already estimated aircraft frequency response using FFT signal analysis as described in "Method II". This amounts to smoothing the noisy frequency response characteristics (at higher frequencies) derived using FFT analysis. The known individual controller transfer functions are then concatenated with the plant transfer functions (Nz/δ_e and q/δ_e) estimated using frequency domain parameter estimation to generate the overall loop transfer function. This method is referred to as "Method III".

The "Method III" was validated using flight simulator responses derived from actual piloted 3-2-1-1 inputs used during the initial flight trials of Light Combat Aircraft (LCA) and is described in [1]. The current paper shares the flight test experience in using "Method III" in near real time for rapid flight envelope expansion. It is found that Methods I and II (qualitative) can be used in conjunction with Method III (quantitative) to predict reliably the available stability margins at various flight conditions.

This paper is divided into six sections. The detailed discussions about the three methods for estimating the margins from flight test data are highlighted in Section **'Three Methods for Stability Margin Estimation using FFT'**. Section **'The Light Combat Aircraft (LCA) and Onboard Flight Test Panel (FTP)'** describes the LCA (Light Combat Aircraft) and the Onboard Flight Test Panel (FTP) used for generating test inputs during LCA flights for flutter and parameter identification. The flight test results are discussed in Section **'Stability Margins Estimation Results from Flight Tests'**. In Section **'Extension of "Method III" for marginal Stability Cases'**, using simulation data it is shown that even if the stability margins are low, they can be reliably estimated using Method III. Section **'Conclusions'** provides the summary and concluding remarks.

Three Methods for Stability Margin Estimation using FFT

A simplified block schematic of a typical aircraft closed loop system for longitudinal axis is shown in Fig.1. The gain and phase margins for the longitudinal axis are calculated analytically by opening the loop at the actuator consolidation point as shown in Fig.1.

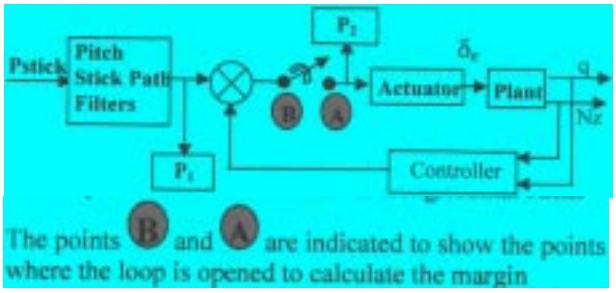

Fig.1 Simplified block schematic of longitudinal axis

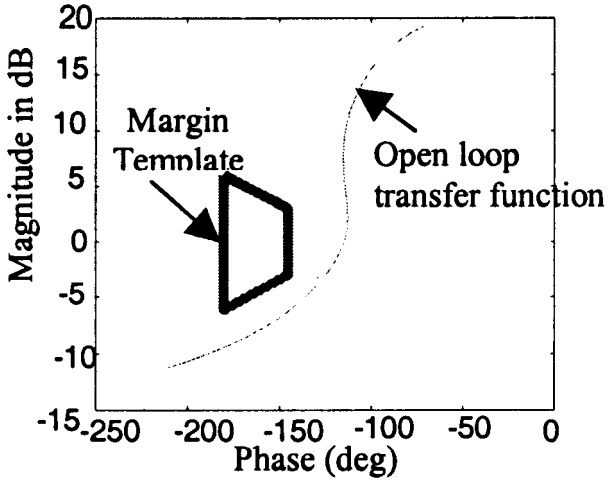

Fig.2 Typical Nichols plot and the stability margin template

The gain and phase margins are distinct stability margin entities. However, for ensuring robustness, the aircraft industry design practice [2] is that the open loop transfer function should not intersect the template in the Nichols plot shown in Fig.2. This is equivalent to meeting both the gain and phase margin requirements simultaneously.

In Fig.1, let the open loop transfer function from "**A**" to "**B**" be denoted by L and the closed-loop transfer function from test points $\mathbf{P_1}$ to $\mathbf{P_2}$ by G. Then by simple algebraic manipulation we can derive L from G as follows:

$$G = \frac{1}{1-L}$$
$$\Rightarrow G - GL = 1$$
$$\Rightarrow L = \frac{G-1}{G} \qquad (1)$$

For an unstable aircraft, it is not possible to open the control loops in flight. Hence, the margins have to be calculated indirectly from the closed-loop responses. Using (1), the open loop transfer function L and hence the stability margins can be determined if one estimates the closed-loop transfer function G from flight test data.

To evaluate the applicability of the stability margin computation methods, the fixed based real time flight simulator of the LCA aircraft called the Engineer-in-loop simulator (ELS) was used as the test platform in [1].To generate the aircraft response trajectories in the simulator, the actual pilot inputs given during the flight tests were injected into the flight simulator after the simulator was trimmed at the reference flight condition. These simulated trajectories were subsequently used for the stability margin calculations.

Method I. Computation of Open Loop Frequency Response from Closed Loop Frequency Response

The ratio of the FFTs of $\mathbf{P_2}$ and $\mathbf{P_1}$ yield the closed loop frequency response $G(jw)$. Using (1) the open loop frequency response is obtained.

The disadvantage of this method is that the bandwidth for an ideal 3-2-1-1 signal of 7 seconds duration is approximately 1 Hz (Appendix A). In addition, a low-pass filter added in the command path of the control laws to meet the handling quality requirements further reduces the bandwidth of the pilot stick input. For a fighter aircraft, the gain margin is generally designed to be greater than 6 dB, and therefore the signal to noise ratio is very low at $\mathbf{P_2}$ (due to signal attenuation). The gain and phase cross over frequencies are of the order of 1 Hz and 3 Hz respectively. Fig.3 shows a typical Nichols plot of the loop transfer function ($L(jw)$) estimated by the above method for ELS data and flight test data. It can be seen that even for the simulated (ELS) data, it is difficult to estimate the margins correctly. For flight-data the estimated Nichols plot is very "noisy" and hence, estimation of gain and phase margins directly with this method is not possible.

Method II. Calculation of the Loop Transfer Function Frequency Response by Concatenating the Estimated Plant Response with the Controller

The digital controller and its associated hardware is generally characterized quite accurately in ground rigs like the ironbird [5]. Using this apriori information, it is necessary to only determine the frequency response of the plant plus actuator from flight test data. The known controller frequency response is then concatenated in series to find the overall open loop transfer function L.

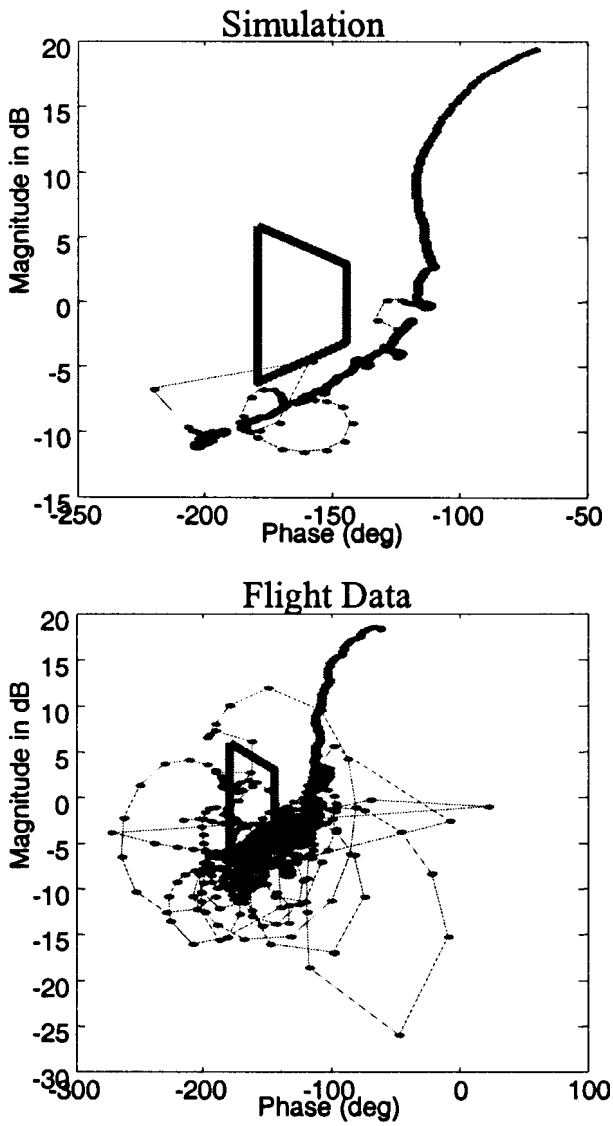

Fig.3 Method I : Nichols plots of Elevon to Elevon transfer function from closed loop (P1 and P2)

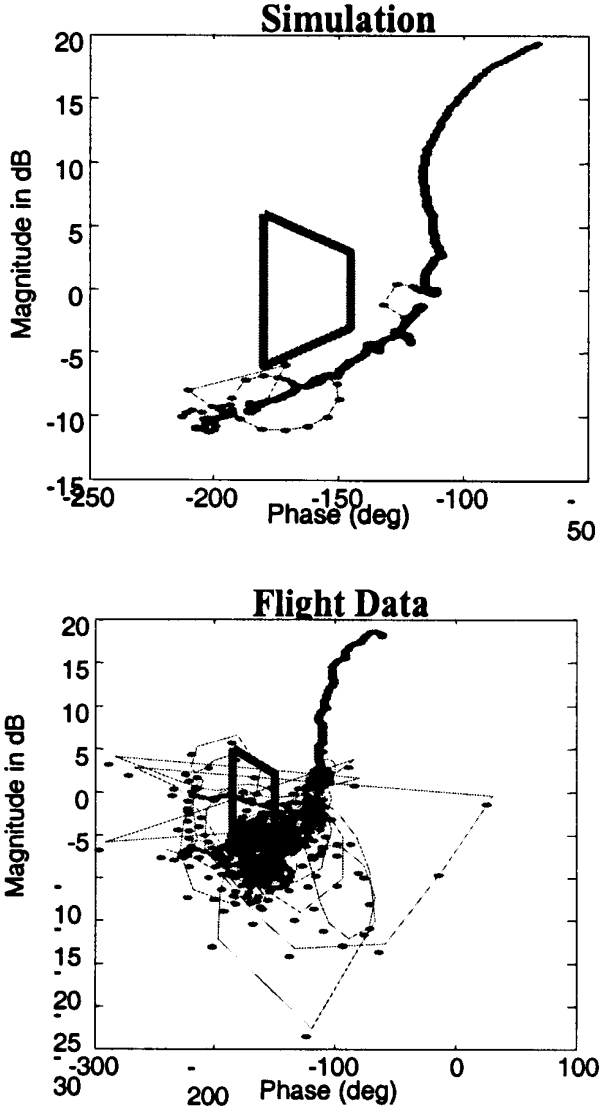

Fig.4 Method II : Nichols plots of Elevon to Elevon transfer function from open loop (q and Nz)

The voted Pitch rate (q), Normal Acceleration (Nz) and elevon command (δ_e) signals (median of multiple sensor signals - is less noisy than the raw signals) are telemetered in real time during the flight tests for subsequent processing.

The ratio of FFTs of q and $\mathbf{P_2}$ and Nz and $\mathbf{P_2}$ yields the plant plus actuator transfer function from $\mathbf{P_2}$ to q and from $\mathbf{P_2}$ to Nz respectively. To this, the known frequency response of the controller is concatenated to obtain the open loop transfer function.

The frequency responses of the loop transfer function for both ELS and flight data are shown in Fig.4, and it can be seen that the results are slightly less noisier compared to those which are obtained from **"Method I"**. However as seen from the Fig. 4, it is still difficult to calculate the margins with this method accurately.

Thus it can be concluded that by just performing a FFT signal analysis of the aircraft response signals, meaningful stability margin estimates cannot be obtained primarily due to the noise in the frequency response data in the 1-4 Hz frequency range. Hence, both Methods I and II are of limited use. From this study, it becomes evident that

some form of smoothing / filtering of the aircraft transfer function responses obtained from the FFT process should be employed. This is the motivation to develop Method III.

Method III. Estimate the Short Period Plant Transfer Function Parameters from the Frequency Responses Obtained in Method II

The structure of pitch rate and normal acceleration transfer functions for symmetric elevon excitation is known a priori, and only the coefficients in the transfer functions are unknown. The short-period approximations for these two transfer functions are as shown below.

$$P_q(s) = \frac{q}{\delta e} = \frac{K_q\left(s + \frac{1}{T_{\theta 2}}\right)}{s^2 + 2\xi_n \omega_n s + \omega_n^2} \tag{2}$$

$$P_{Nz-cg}(s) = \frac{Nz_{cg}}{\partial e} = \frac{K_{nz}\left(s + \frac{1}{T_{h2}}\right)\left(s + \frac{1}{T_{h3}}\right)}{s^2 + 2\xi_n \omega_n s + \omega_n^2} \tag{3}$$

$Nz_{sensor} = Nz_{CG} + \dot{q}x_s$, Where, x_s is the forward displacement (in meters) of the accelerometer sensor from the CG in the x direction.

$$P_{Nz}(s) = \frac{Nz_{sensor}}{\delta e}$$

$$= \frac{K_{nz}\left(s + \frac{1}{T_{h2}}\right)\left(s + \frac{1}{T_{h3}}\right) + x_s\left(\frac{\pi}{180}\right)K_q\, s\left(s + \frac{1}{T_{\theta 2}}\right)}{s^2 + 2\xi_n \omega_n s + \omega_n^2} \tag{4}$$

The elevon actuator transfer function is obtained from rig tests. The frequency response of this actuator transfer function along with the onboard computer computation delay of 8 ms modeled as a transportation lag is cascaded with the frequency response of $P_q(s)$ and $P_{Nz}(s)$ to obtain the frequency response from $\mathbf{P_2}$ to q and Nz.

Let $\alpha = 2\xi_n\omega_n$, $b = \omega_n^2$, $z_{\theta 2} = 1/T_{h2}$ and $z_{Th3} = 1/T_{h3}$. Now, (2) and (4) have seven unknown variables. These seven variables can be rearranged in the vector form as

$$X = \left[K_q,\, Z_{\theta 2},\, a,\, b,\, K_{Nz},\, Z_{Th2},\, Z_{Th3}\right] \tag{5}$$

To facilitate fast convergence during optimization in real-time, bounds on the parameters in X are established a-priori. Upper and lower bounds on the parameters in X are obtained from the wind tunnel data based aircraft model used in the simulator as follows.

The scatter in these seven parameters at various flight conditions due to variation in aircraft mass and c.g. can be determined from the linear models generated at these flight conditions. A 2-D look-up table (as a function of Mach and altitude) corresponding to the mean values of the parameters is then generated. The scatter is then expressed as a percentage variation over and above the mean value. Since, these parameters are estimated from wind-tunnel data, there is some more uncertainty, hence an additional ±10% over and above this variation is added for computing the parameter bounds.

Let the frequency responses obtained from the flight test data over a frequency range [$w1$, $w2$] from $\mathbf{P_2}$ to q and Nz be denoted as $F_{q[w1,w2]}$ and $F_{Nz[w1,w2]}$ respectively. Then the problem reduces to finding the optimum parameter vector X^* which minimizes a cost function - defined as the root sum square of the error between the frequency response obtained from the flight data and the aircraft model as postulated in (2) and (4) denoted by $P_{q[w1,w2]}$ and $P_{Nz[w1,w2]}$ respectively. The best-fit q and Nz transfer functions are derived by optimizing the following cost function.

$$\min_{x \in [X_{lower},\, X_{upper}]} \sqrt{\left|F_{q[w1,w2]} - P_{q[w1,w2]}\right|^2 + \left|F_{Nz[w1,w2]} - P_{Nz[w1,w2]}\right|^2} \tag{6}$$

The resulting analytical aircraft q and Nz transfer functions obtained by substituting the seven parameters after optimization are then used for computing the open loop transfer functions, and subsequently the stability margins.

Validation of "Method III" using 'Offline' Canned Inputs (ELS Simulation)

The accuracy of the margins computed by "Method III" is verified by generating the linear perturbation models ('Truth Model') at the reference flight conditions for the aircraft using the six-degree of freedom non-linear data. The stability margins are computed analytically by concatenating the digital controller with the linear models and considering all the other dynamic elements in the

closed loop system. These stability margins are used as a reference for comparing the results generated using "Method III" from simulated time response output signals. The procedure for computing the stability margins using 'Method III' consists of the following steps.

- Trim the flight simulator to the reference flight condition.
- Generate the aircraft model (ELS) responses by injecting the pilot 3-2-1-1 input into the simulator. Record $\mathbf{P_1}$, $\mathbf{P_2}$, *q*, and *Nz* time responses.
- Perform FFT signal analysis on these time domain signals and compute aircraft transfer functions using 'Method II'.

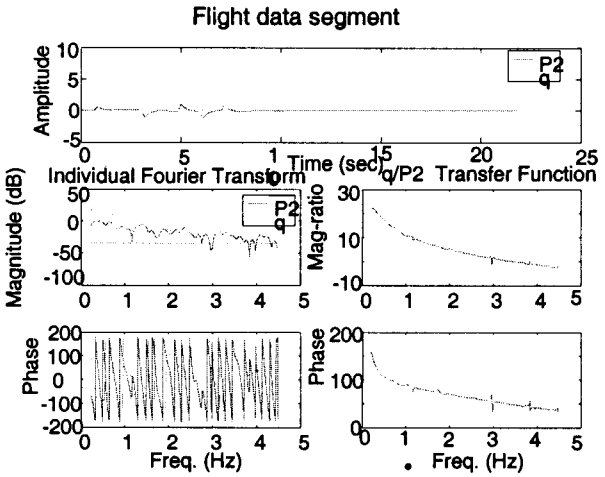

Fig.5 Individual and ratio of fourier transforms of pitch rate and P2

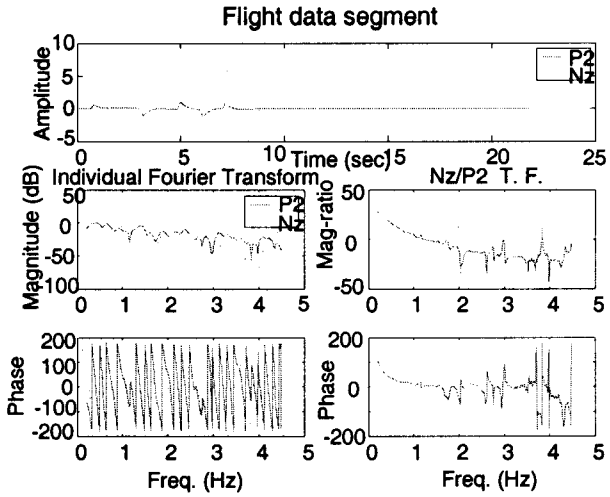

Fig.6 Individual and ratio of fourier transforms of normal acceleration and P2

- Estimate the 'best' *q* and Nz transfer functions for the aircraft using the optimization criterion given in (6).

The pilot inputs used for this verification / validation process were extracted from the pilot generated 3-2-1-1 segments in actual flight.

Figure 5 shows the time response for $\mathbf{P_2}$ (which is the equivalent δe command) and pitch rate (*q*) signal after removing the bias. For both these signals, Fourier Transform is plotted in terms of magnitude and phase up to 4.5 Hz. The dotted horizontal straight line at -35db indicates the frequencies at which the magnitude spectrum for $\mathbf{P_2}$ lies above this line and only these segments are considered for optimization. The ratio of pitch rate magnitude spectrum to that of $\mathbf{P_2}$ is also plotted. The phase difference between these two signals is plotted in the bottom right graph.

Similarly, in Fig.6, $\mathbf{P_2}$ and *Nz* data are plotted. Since *Nz* is the acceleration signal it is noisier than the pitch rate signal, the requirement of excitation level to get reliable output data from *Nz* was found to be higher when compared to pitch rate. The dotted horizontal straight line at -20db in Fig.6 indicates the frequencies at which the magnitude spectrum for $\mathbf{P_2}$ lies above this line and only these segments are considered for optimization. The cut-off levels of -35dB for *q* (Fig.5) and -20 dB (Fig.6) for *Nz* were arrived at based on detailed studies across various flight segments.

Figure 7, shows the *q* and *Nz* frequency response obtained from linear models in Methods II and III. The smoothing of the noisy data in Method III is quite apparent. In the normal acceleration transfer function; Method III frequency response starts to deviate from the linear model beyond 2Hz. This can be attributed to the lower signal to noise ratio in the accelerometer signal. In Fig. 8,

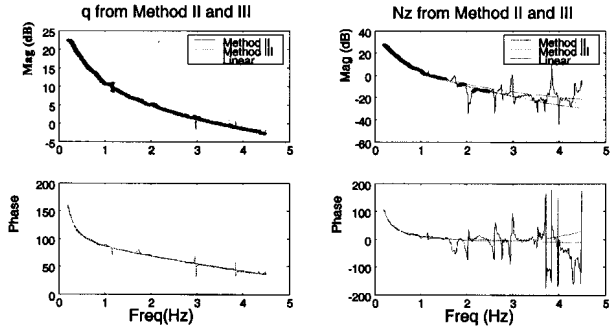

Fig.7 Pitch rate and normal acceleration transfer functions from Method II and III

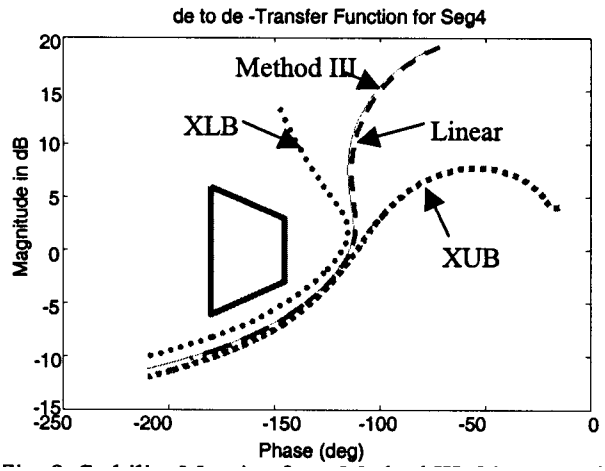

Fig.8 Stability margins from Method III, Linear model, Upper (XUB) and Lower (XLB) bounds (Simulation)

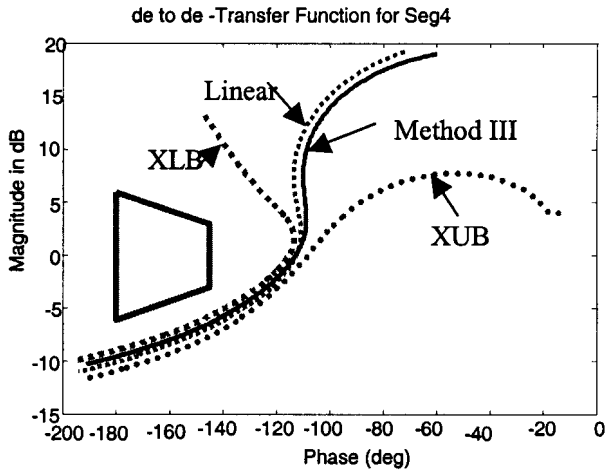

Fig.9 Stability margins from Method III, Linear model, Upper (XUB) and Lower (XLB) bounds (Flight data)

Table-1 : A comparison of gain and phase margins results (method III-Simulation)

	Gain Margin (dB)			Phase Margin (deg)		
	Estimated	Linear	Error	Estimated	Linear	Error
Seg 1	-9.9017	-9.9303	0.0286	65.2539	64.6142	0.6397
Seg2	-17.3126	-16.1655	-1.1471	64.1585	62.6335	1.525
Seg3	-17.3291	-16.3540	-0.9751	60.3994	62.8047	-2.4053
Seg4	-11.9198	-11.0773	-0.8425	64.4464	64.6009	-0.1545
Seg5	-0.4669	-8.8653	-0.6016	62.7561	62.6806	0.0755
Seg6	-9.8986	-9.4314	-0.4672	58.5817	57.9366	0.6451
Seg7	-12.9386	-13.2157	0.2771	58.9112	56.7044	2.2068
Seg8	-16.5740	-16.6743	0.1003	62.5875	63.0421	-0.4546
Seg9	-9.9611	-9.5612	-0.3999	63.9688	64.2679	-0.2991
Seg10	-9.3749	-9.3520	-0.0229	65.1023	64.8873	0.215
Seg11	-13.3430	-13.2820	-0.0610	58.077	57.394	0.683
Seg12	-11.6093	-11.4111	-0.1982	59.913	58.4677	1.4453

the loop transfer functions for Method III and the nominal linear model are plotted. The Nichols plots of the loop transfer function generated using the upper and lower bounds (used in optimization) of the parameter vector *X* are also plotted. From Fig. 9, it can be seen that gain and phase margins of Method III and nominal linear model match very well and thus validating the proposed method. The values of gain and phase margins are compared in Table-1 for various flight-test segments.

The maximum absolute error in estimation of stability margin is 1.14dB (Seg2) in magnitude and 2.4058 deg in phase (Seg1). For both these data segments, in frequency domain, the magnitude spectrum is lower in gain when compared to the other segments.

"Method III" Applied to Flight Data

Twelve typical 3-2-1-1 input segments generated manually by the pilot at various flight conditions are used in this study. "Method III" is used to estimate stability margins from flight test data for all the above flight test segments.

Figure 9 also shows the comparison of estimated margins with the margins obtained from a linear model at the same flight condition and mass / C.G configuration for the flight segment 'Seg4'. The Nichols plots of the loop transfer function generated using the upper and lower bounds (used in optimization) of the parameter vector X are also plotted. The estimated Nichols plot falls within bounds, which confirms the estimated values have not saturated at the extreme boundary values during optimization.

The margins estimated from flight data for all twelve data segments along with margins obtained from linear models corresponding to the "closest" fuel state in flight are tabulated in Table-2.

For the estimates generated from flight-test data the worst deviation from the linear models is 1.2840 dB in gain and 3.9489 deg in phase. The difference between flight estimated and model predicted stability margins can be mainly attributed to (among other errors):

- Inaccuracy of aerodynamic parameters, which are based on wind tunnel data.
- The fuel state used for generation of linear models is not exact; it is approximated to the "closest" Flight Fuel state for which data is available.
- Accuracy of mass / inertia / C.G data

Despite all these real world effects, the estimated gain and phase margins are quite close to the ones obtained from linear models. This establishes a high degree of confidence in the non-linear simulation model (used for control law design) as being a satisfactory representation of the actual aircraft in the flight envelope tested. Thus, Method III can be used with confidence for near real time estimation of gain and phase margins and can be a useful tool for rapid envelope expansion in subsequent flight test programs.

The Light Combat Aircraft (LCA) and Onboard Flight Test Panel (FTP)

India's LCA is a single engine tail-less delta wing supersonic fighter aircraft, which is designed to be aerodynamically unstable in the longitudinal axis. LCA is stabilized artificially and the desired performance is achieved over the entire flight envelope using a quadruplex redundant full authority digital Fly-By-Wire (FBW) Flight Control System (FCS). The control laws resident in the sophisticated electronic FBW-FCS in addition to guaranteeing stability, optimize the aircraft performance and piloted handling qualities over the entire flight envelope for all aircraft external store configurations. An overview of the design, development and testing of the flight control laws for the LCA is given in [5].

The Flight Control System (FCS) Test Panel (FTP) is primarily a programmable function generator provided on board the aircraft to generate synthetic inputs of pre-de-

Table-2 : Estimation gain and phase margins using Method III foir flight data

	Gain Margin (dB)			Phase Margin (deg)		
	Estimated	Linear	Error	Estimated	Linear	Error
Seg 1	-10.2918	-10.6329	0.3411	67.4739	66.6374	0.8365
Seg2	-15.5944	-16.8779	1.2835	67.6685	63.7191	3.9494
Seg3	-16.443	-17.0731	0.6301	65.1447	63.8923	1.2524
Seg4	-10.9988	-11.7865	0.7877	67.1017	66.3592	0.7425
Seg5	-9.2921	-9.5741	0.282	63.4129	65.0841	-1.6712
Seg6	-10.1698	-10.1517	-0.0181	58.5579	60.178	-1.6201
Seg7	-13.6748	-13.9331	0.2583	61.3063	58.0451	3.2612
Seg8	-17.1045	-17.3915	0.287	65.4204	64.0123	1.4081
Seg9	-9.9429	-10.2764	0.3335	63.9442	66.3102	-2.366
Seg10	-9.2971	-10.061	0.7639	66.1734	67.1342	-0.9608
Seg11	-14.7228	-14.0023	-0.7205	58.216	58.8527	-0.6367
Seg12	-12.7666	-12.1571	-0.6095	62.6297	60.214	2.4157

fined characteristics. Pilot can select a particular input that is to be injected at specific points within the DFCC (Digital Flight Control Computer) for parameter identification and flutter tests. The DFCC receives inputs from the FTP through either of two communication channels, one simplex digital RS-422 serial link for parameter identification purposes and the other through a set of five analogue lines (four elevons and one rudder) for carrying out flutter/structural coupling tests. Programming of the function generator in flight is made pilot-friendly by utilizing a pre-programmed EPROM containing predefined data for a maximum of 100 (0 to 99) test-points.

The pilot initiates each run by selecting a pre-programmed maneuver using buttons on the FTP panel inside the cockpit. The pilot trims the aircraft straight and level at the desired flight condition, and the engage / disengage button on the FTP is then used to initiate the test maneuver. Based on the experiment selected desired inputs like doublets, 3-2-1-1 etc. are added from FTP in digital form to the appropriate forward path of the control law for parameter identification. On the other hand, analog impulse, sine sweep inputs are added from FTP directly to the actuator command to drive the control surfaces for exciting the structural modes. In both the cases, the feedback control system is still in operation. The excitation can be stopped by the pilot toggling the engage/disengage button, or by moving the stick/rudder, or automatically by the DFCC software, which has a provision to abort the test in case of pre-defined safety criteria being violated. The pre-defined safety criteria are mainly based on 'g'-limits, actuator rate and position limits, feedback sensor and pilot input (stick/pedal) limits.

On completion of the test sequence the programme resident in a desktop computer connected to the telemetry system carries out the optimization and plots the estimated open loop frequency response in Nichols plot using Method I, Method II and Method III. From Fig.10, it can be noted that the loop transfer function obtained from flight data using Method I and II is very noisy in the gain and phase cross over frequency regions. However, the good match at lower frequency between all three methods gives a confirmation that the stability margins estimated using Method III are correct. Thus, 'qualitative' results from Method I and II are used to confirm the 'quantitative' results for stability margin estimation using Method III as shown in Fig.11. Along with the estimated stability margins plots, the stability margins obtained from equivalent linear models for the same trim conditions are also plotted. The whole process takes less than a 'minute'.

During this time, Pilot carries out PID inputs in other axis or flutter inputs at the same Mach-altitude test point. Immediately after confirmation of the stability margins, the Pilot is given a clearance to carry out the next test point.

Stability Margins Estimation Results from Flight Tests

The control law development process for the LCA was planned in a progressive manner. For the initial flights (First block) of the Technology Demonstrators TD-1/ TD-2, since angle of attack, sideslip and airdata (Pt, Ps) information was not available (pending flight calibration)

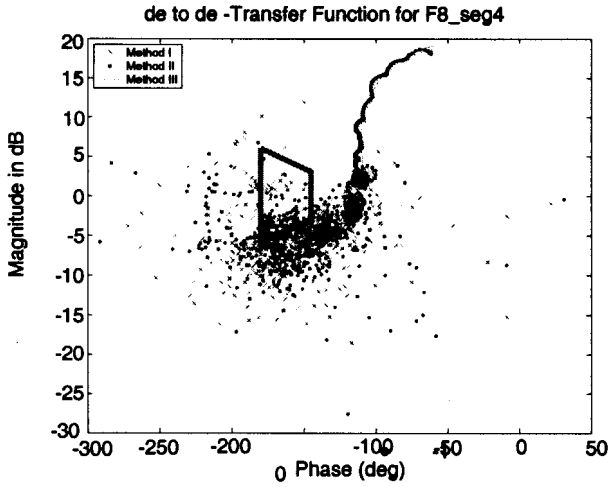

Fig.10 The qualitative results from Method I and II can be used to establish the confidence in the quantitative results from Method III

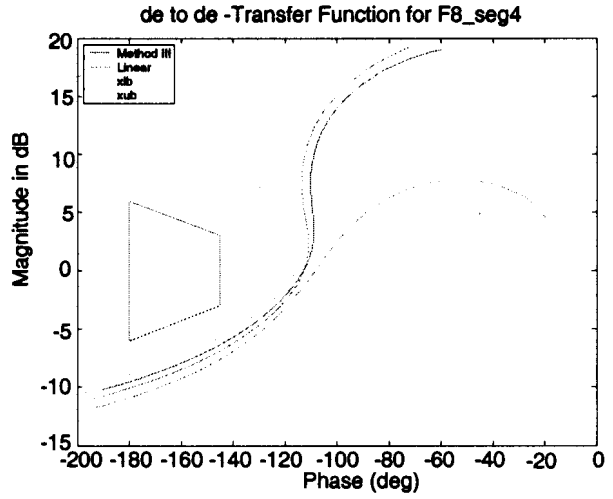

Fig.11 Stability margins from Method III, linear model and upper and lower bounds (from flight data)

to the control laws, they were operated in the 'fixed gain' mode over a *restricted flight envelope* using only signals from the inertial sensors (rate gyros and accelerometers). As the dynamic pressure increases the plant gain increases and hence one must proportionately reduce the controller gain so that total loop gain remains same. This ensures that the desired performance is obtained throughout the dynamic pressure range. However, if one chooses the fixed gain controller as shown in Fig.12, then the gain margin starts reducing as the dynamic pressure increases and hence the aircraft can be flown only in a 'restricted flight envelope'.

During the LCA first block of flights, manual 3-2-1-1 and doublet inputs were applied for conventional parameter estimation analysis. The computer generated signal injection system capable of exciting the aircraft with signals such as i) sine sweep signals or ii) higher bandwidth 3-2-1-1 signals was not cleared for first block of flights. Due to this restriction and limited flight test time, sine sweep inputs, which would have been more suitable for stability margin estimation, were not applied. Typical flight test results and comparisons of the flight responses with simulator results are given in [5]. While good match in time responses gave the control law designers reasonable confidence in the wind tunnel data based flight models used for design, it was still necessary to establish the available stability margins by computing the loop transfer functions from flight data.

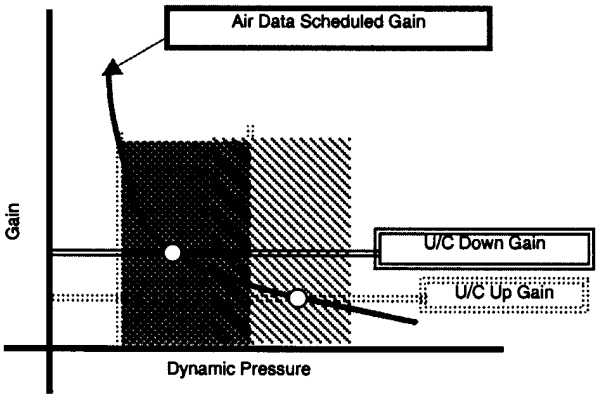

Fig.12 Optimum fixed gain selection

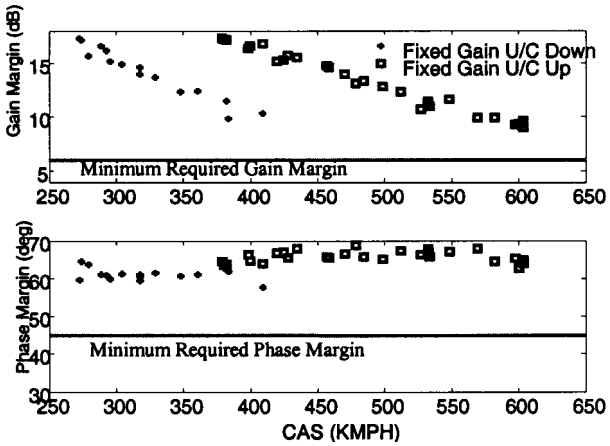

Fig.13 Estimated gain and phase margins from flights

The focus of these tests was towards validating the aerodynamic data set used for design, calibration of the air-data system and evaluation of the aircraft's performance. This enabled use of airdata for scheduling the control law gains during the subsequent block of flights and expansion of the flight envelope.

The gain and phase margins estimated in near real time using Method III for fixed gain control laws are presented in Fig.13. It can be seen that as the CAS increases the gain margin reduces since the controller gains are fixed and depend on the undercarriage position as illustrated in Fig.12. Moreover, around 370 KMPH a sudden increase in gain margin can be seen. This is because the gains are reduced when undercarriage is retracted (i.e. down to up).

Figure 14 shows the Fixed gain 'Undercarriage Down' (FG DN) and 'Undercarriage Up' (FG UP) flight enve-

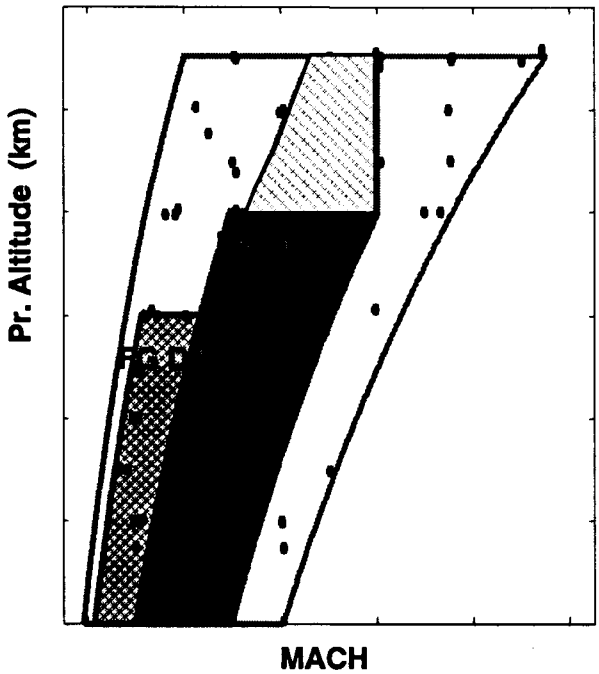

Fig.14 Flight envelope

lope. Subsequently, the flight envelope was expanded to higher altitudes as shown in this figure with the fixed gain CLAW UC Up mode. This clearance was based on the good stability margins obtained from the flight tests. The expansion was required to test other aircraft subsystems at higher altitudes.

Once the airdata and angle of attack sensors were flight calibrated over the 'restricted flight envelope' in first block of flights, a 'scheduled gain' claw version with back up mode as 'fixed gain' was flown in the second block of flights.

The Gain margins estimated in scheduled gain flights for various CAS and Mach are shown in Fig.15. It can be noticed that in Fig.15 as CAS increases the gain margin does not reduce since the feedback gains are scheduled as a function of Mach and altitude so that a uniform gain margin is obtained throughout the flight envelope.

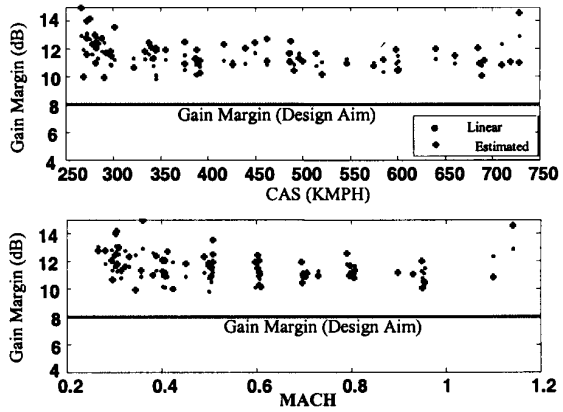

Fig.15 Estimated margins from flights (SGSB)

Extension of "Method III" for Marginal Stability Cases

During LCA flights, the stability margins were found to be satisfactory throughout the flight envelope. To know how "Method III" would perform when the stability margins were poor, a simulation study was carried out. A block Ke^{-sT} is introduced in Fig.1 between "actuator" and "plant" transfer function blocks to vary the plant gain or add a phase delay by changing K and T respectively. By increasing the plant gain K or phase delay T in the simulation model it is shown that even if the stability margins are low "Method III" correctly estimates the margins. Obviously, if the system becomes unstable then it is not possible to estimate the margins.

Using the piloted 3-2-1-1 input, six DOF simulation data was generated by varying K and T for the following three cases

1. Vary T with K constant (set K=1),
2. Vary T with K constant (set K=1.5),
3. Vary K with T constant (set T=0)

These results are tabulated in Tables-3 to 5. Tables-3 to 5, confirm that the estimated margins are satisfactory even when margins are much lower than the desired 6dB-35° template. Methods I and II are useful in establishing the confidence in the results obtained in the above tables from Method III .

Conclusions

This paper addresses the estimation of stability margins for the Light Combat Aircraft (LCA) in near real time. LCA is a longitudinally unstable Fly-by-wire aircraft. Hence estimation of stability margins, especially in the longitudinal axis, during the initial flight tests of this new

Table-3 : Constant gain (K=1) and variable T

T	From ELS Replay with K=1					
	Gain Margin (dB)			Phase Margin (deg)		
	Estimated	Linear	Error	Estimated	Linear	Error
0.0125	8.3559	8.2993	0.0565	60.6371	60.3135	0.3235
0.0500	5.7319	5.6583	0.0735	46.9088	46.4816	0.4272
0.100	3.1154	3.0237	0.0917	28.5453	28.0391	0.5062
0.1375	1.5664	1.4495	0.1169	15.0279	14.2072	0.8207
0.1500	1.1473	0.9834	0.1639	10.9601	9.5966	1.3635
0.1625	0.8030	0.5171	0.2859	7.4898	4.9859	2.5039

Table-4 : Constant gain (K=1.5) and variable T

T	From ELS Replay with K=1.5					
	Gain Margin (dB)			Phase Margin (deg)		
	Estimated	Linear	Error	Estimated	Linear	Error
0.05	2.2032	2.1365	0.0667	23.0812	22.5180	0.5632
0.075	0.8190	0.7304	0.0886	8.8704	7.8628	1.0075

Table-5 : Variable gain K and Constant T (T=0)

K	From ELS Replay with T=0					
	Gain Margin (dB)			Phase Margin (deg)		
	Estimated	Linear	Error	Estimated	Linear	Error
1.5	5.8796	5.8331	0.0465	52.1494	51.8285	0.3209
2	3.3701	3.3343	0.0358	35.6551	35.3517	0.3033
2.5	1.3506	1.3961	-0.0455	16.3959	16.8702	-0.4743
2.8	0.1039	0.4117	-0.3078	0.5866	4.8055	-4.2189

aircraft was important to gain confidence and establish the accuracy of the flight model used for control law design.

The method for estimating the gain and phase margins, in near real time, proposed by authors [1] has been successfully used for flight envelope expansion of LCA. This method uses only the aircraft response signals to pilot applied 3-2-1-1 inputs or FTP generated 3-2-1-1 inputs, which do not have a sufficiently high spectral content. The two step method consists of first determining the aircraft parameter frequency responses using FFT signal analysis followed by estimation of analytical transfer functions of the aircraft from the FFT derived frequency response.This procedure essentially smoothens the FFT derived frequency response, especially near phase cross over frequencies, enabling reliable estimation of both gain and phase margins.

The stability margins for LCA are estimated at various flight conditions in near real time during LCA flights.The stability margin estimation indicates that the flight model of the LCA simulator derived from wind tunnel aerodynamic data and all other pertinent aircraft data is a close representation to the actual aircraft. Thus, the stability margins predicted prior to flight have been achieved in the actual flights of the LCA in the flight envelope tested.

During the LCA flights, the stability margins were found to be satisfactory throughout the intended flight envelope. In order to establish that the same technique would work when the stability margins were marginal, the plant gain was artificially increased and a synthetic delay was added in the simulation model. The margins were estimated and it is shown that even if the stability margins are low the same technique correctly estimates the relative stability. In fact, the signal-to-noise ratio is better when the stability margins are lower due to the ‘higher plant gain’ and the ‘lower crossover frequencies’. It is shown in this paper that "Method III" can be used reliably even up to the point of instability.

Acknowledgement

The authors wish to acknowledge the support given for this work by the Scientists of National Aerospace Laboratories (NAL), Aeronautical Development Agency (ADA), Aeronautical Development Establishment (ADE), Hindustan Aeronautics Limited (HAL) and the Test Pilots and Engineers from the National Flight Test Centre (NFTC), ADA. The authors also thank the Directors of NAL and ADA for their constant encouragement and permission to publish this paper.

References

1. Vijay V. Patel., Girish Deodhare. and Shyam Chetty., "Near Real Time Stability Margin Estimation from Piloted 3-2-1-1 Inputs", AIAA Aircraft

Technology Integration and Operations (ATIO2002) Technical Forum, Los Angeles, CA, October 2002.

2. Smith, T., "Ground and Flight Testing of Digital Flight Control Systems", Chapter 6, Flight Control Systems, Edited by Roger W. Pratt, Progress in Astronautics and Aeronautics, Vol.184, Paul Zarchan, Editor-in-Chief, 2000.

3. Mark B. Tischler., "System Identification Methods for Aircraft Flight Control Development and Validation", Chapter 2, Advances in Aircraft Flight Control, Taylor and Francis, 1996.

4. Peter G. Hamel. and Ravindra Jategaonkar., "Evolution of Flight Vehicle System Identification", Journal of Aircraft, Vol. 33, No.1, January-February 1996, pp. 9-28.

5. Shyam Chetty., Girish Deodhare. and B. B. Misra, "Design, Development and Flight Testing of Control Laws for the Indian Light Combat Aircraft", AIAA Conference on Guidance, Navigation and Control, 2002.

6. Alan V. Oppenheim. and Ronald W. Schafer., Digital Signal Processing, Prentice Hall, 1989.

7. McRuer D. Ashkenas. and Graham, D., Aircraft Dynamics and Automatic Control, Princeton, New Jersy, 1973.

8. Robert Clarke., John J. Burken., John T. Bosworth. and Jeffery E. Bauer., "X-29 Flight Control System: Lessons Learned", NASA Technical Memorandum 4598, June 1994.

9. John T. Bosworth. and John J. Burken., "Tailored Excitation for Multivariable Stability-Margin Measurement Applied to the X-31A Nonlinear Simulation", NASA Technical Memorandum 113085, August 1997.

10. Nanson, K.M. and Ramsay, R.B., "The Development and Use of in-flight Analysis at BAE Warton", Advances in Flight Testing, AGARD-CP-593, December 1997.

Appendix A :- Fourier Transform of 3-2-1-1 Signal

Remark 1: If the period T is halved the frequency bandwidth doubles and the magnitude of the spectrum halves. Thus, even though the bandwidth increases, excitation level decreases as T reduces.

Remark 2 : With 3-2-1-1 input for T=1, at 1 Hz there is no excitation to the plant (which is approximately the gain cross over frequency).

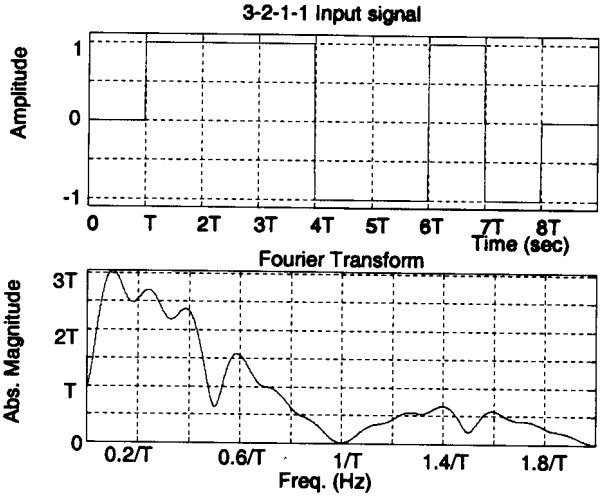

Fig.A1 : Normalized fourier transform for 3-2-1-1 input